ELSEVIER

Journal of Power Sources 87 (2000) 137–143

JOURNAL OF POWER SOURCES

www.elsevier.com/locate/jpowsour

Lead electrowinning in a fluoborate medium. Use of hydrogen diffusion anodes

E. Expósito, J. González-García, P. Bonete, V. Montiel, A. Aldaz *

Departamento de Química Física, Universidad de Alicante, Grupo de Electrquimicq Aplicada, Ap. Correos 99, 03080 Alicante, Spain

Received 10 June 1999; accepted 4 October 1999

Abstract

The results of an investigation of the electrowinning of lead employing a fluoboric acid bath are reported. The electrodeposition lead reaction was studied by voltammetric methods and scanning electron microscopy (SEM) microphotographs of the electrodeposited lead were taken. The effects of current density, temperature, catholyte flow and H^+ concentration were investigated on a laboratory scale to optimise operating conditions. Finally, the substitution of the traditionally used Dimensionally Stable Anode (DSA) by a Hydrogen Diffusion Electrode (HDE) was made in order to decrease the energy consumption (EC) of the overall process.

Keywords: Lead; Electrowinning; Hydrogen diffusion anode; Fluoborate bath

1. Introduction

Within the next few years, the percentage of recycled lead acid batteries in the European Community must increase to almost 100%, in agreement with new regulations. At the moment, the recycling of lead content in batteries is carried out by pyrometallurgical processes [1]. However, these processes have important problems. Firstly, emissions of lead and SO_2 fumes during pyrometallurgical smelting are very hard to control and it will be difficult and costly to meet the emission and ambient air standards promulgated by environmental organisations. Second, the lead obtained must be of a high purity to be suitable for producing maintenance-free batteries [2].

For these reasons, in the last two decades there has been an increasing effort to recycle lead from scrap batteries using electrolytic methods [3–9]. These processes consist in a three-step treatment. After a first step for breaking the batteries and separating the plastic compounds and grids, the next step includes the hydrometallurgical processing of scrap batteries. At the end of this stage, a solution with a high concentration of Pb^{2+} ions is obtained. Fluoboric, fluosilicic and hydrochloric acids together with ammonium sulphate have been used as electrolytes. It is interesting to note the Ginatta Process [9], which deals with the electrowinning of lead from a fluoboric acid solution. The last step is the electrowinning of lead in order to obtain it in metallic form.

In the frame work of a 3-year EC programme, a team of five research laboratories of European enterprises and universities have studied the development of a new process for the recycling of lead from scrap batteries in chloride solution [8].

The anodes usually employed in these hydrometallurgical lead recovery processes are principally Oxygen Dimensionally Stable Anodes, DSA-O_2 or Pb–Ag alloys. On these anodes and in acidic medium, the anodic reaction is the oxidation of water:

$$2H_2O \Leftrightarrow O_2 + 4H^+ + 4e^- \quad E^0 = 1.23 \text{ vs. NHE.} \qquad (1)$$

One of the main problems in using DSA-O_2, in lead containing solutions is the poisoning of the anode by formation of an insoluble deposit of lead dioxide according to the reaction:

$$Pb^{2+} + 2H_2O \rightarrow PbO_2 + 4H^+ + 4e^-. \qquad (2)$$

The lead dioxide formation decreases the quantity of lead recovered in metallic form, shortening the lifetime of the DSA-O_2 anode. This problem can be partially pre-

* Corresponding author. Tel.: +34-6590-3536; fax: +34-6590-3537; e-mail: dgfis@ua.es

0378-7753/00/$ - see front matter
PII: S0378-7753(99)00438-3

vented by adding small amounts of arsenic [4] or phosphoric acid [10] or using a divided cell.

Another possibility to avoid the problem caused by lead dioxide formation and, at the same time, to diminish the energetic cost of the process is the use of Hydrogen Diffusion Electrodes (HDE) as anodes in lead electrowinning. The working potential of a HDE anode is low enough to prevent PbO_2 formation, allowing the use of an undivided cell.

Hydrogen and Oxygen Diffusion Electrodes were developed as electrodes for fuel cells [11–13]. This type of electrode is usually made up of a semihydrophobic composite of catalysed high surface area carbon and a fluorocarbon binder that are thermally sintered onto or into a planar substrate. The substrate materials of choice are normally carbon cloth, carbon paper, metallic mesh or expanded metal. It is desirable to achieve very fine porosity in order to form a three-phase interface of very high surface area. HDE have been previously employed in Zn [14,15] and Ni [16] electrowinning processes and in Pb removal in wastewater [17].

The anodic reaction taking place at a HDE is the oxidation of H_2:

$$H_2 \rightarrow 2H^+ + 2e^- \quad E^0 = 0.00\,V \text{ vs. NHE.} \qquad (3)$$

Thus, the change of the oxygen evolution reaction by the hydrogen oxidation reaction decreases the thermodynamic cell voltage by 1.23 V at standard temperature and pressure. Taking into account that the oxygen evolution reaction is more sluggish than hydrogen oxidation, the real voltage saving should in fact be greater. In order to translate this voltage saving to cost saving, the price of the hydrogen employed to feed the HDE must obviously also be taken into account.

In this paper, the electrodeposition of lead in a fluoroborate medium was investigated from a fundamental and applied point of view. First, the deposition process was studied by means of cyclic voltammetry, scanning electron microscopy (SEM) and EDX. This study was followed by a more applied one in which parameters such as current efficiency (CE) and the physical properties of the lead deposit were optimised. Finally, a comparative study of the advantages of using a HDE instead of traditionally used DSA-O_2 was also made.

2. Parameters of interest

2.1. Current efficiency

CE is the percentage of electrical charge used for the desired reaction relative to the total charge passed.

$$CE\% = \frac{\text{Charge used for the deposit of lead}}{\text{Total charge passed}} \times 100 \qquad (4)$$

2.2. Energy consumption (EC)

This parameter can be defined as the energy necessary to obtain a given amount of product. Normally, it is expressed in kW h per kg of product obtained.

$$EC\left(\frac{kW\,h}{kg\,B}\right) = \frac{2680.55 \times E_{cell}}{M_B \times CE\% \times \frac{b}{n}} \qquad (5)$$

where M_B is the molecular weight of B (g/mol), b is the stoichiometric coefficient of B, n is the number of electrons and E_{cell} is the cell voltage (V).

3. Experimental

3.1. Voltammetric study

Electrochemical experiments were made in a VOLTALAB-32 RADIOMETER system. The SEM and EDX analyses were carried out with a Link X-ray Analytical System

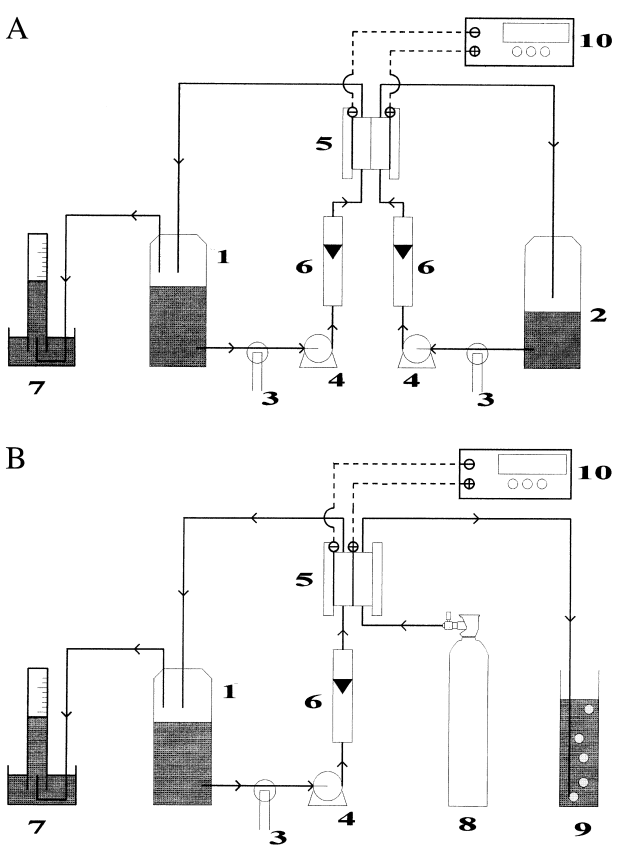

Fig. 1. Schematic illustration of the electrochemical process using (A) DSA-O_2 anode and (B) HDE anode. 1 — Catholyte reservoir. 2 — Anolyte reservoir. 3 — Heat exchanger. 4 — Pump. 5 — Filter press reactor. 6 — Flowmeter. 7 — Hydrogen volume measurement system. 8 — Hydrogen feed. 9 — Water column for hydrogen overpressure. 10 — Power supply.

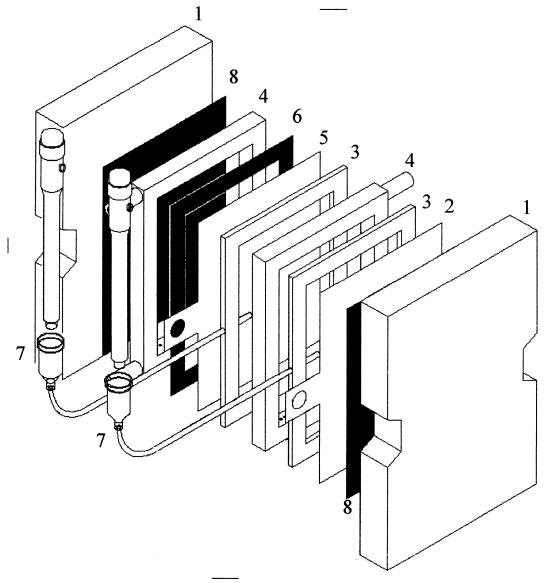

Fig. 2. Scheme of a filter press cell using a HDE anode. 1 — End plates. 2 — Cathode. 3 — Silicon gasket. 4 — Compartment frame. 5 — HDE anode. 6 — Rubber gasket. 7 — Reference electrode. 8 — Insulator gasket.

model QX200. Solutions were prepared with ultrapure water from a MilliQ system. The reactants employed were, HBF_4 48% from Aldrich, PbO > 99% of purity from Fluka, H_3BO_3 99% of purity from Sigma. Before each experiment, solutions were deaerated by bubbling N_2 quality N-50 from L'Air Liquide. The working electrode was a Cu rod (Goodfellow, diameter 2.9 mm, purity 99.99%). Before each experiment, it was polished and cleaned by standard procedures. The counter electrode was made of Pt, and the reference electrode was a SCE Tacussel, model TR-100. Unless stated otherwise, all potentials will be referred to SCE. Solution composition and scan rate were in all cases 0.48 M HBF_4 + 0.16 M H_3BO_3 + 0.48 M Pb^{2+} and 0.05 V/s, respectively.

3.2. Laboratory scale plant

Schematic diagrams of the laboratory plant and the filter press reactor are shown in Figs. 1 and 2. Although filter press type reactors are not appropriated for their use in electrowinning, this reactor was chosen as it has very uniform potential and current distributions, defined flow patterns, etc. In this way, it allowed us to obtain great reproducibility in our results. Moreover, with this reactor, the measurement of the amount of H_2 evolved can be carried out with high precision and it is adequate if HDE anodes are used. Finally, the multi-electrode cells developed in the LEREFLEOS European Project [8] have flow patterns very similar to those of a filter press.

The cathode was a Cu sheet. Metakem supplied the DSA-O_2 anode and the HDE was home-made [17]. The separator was a perfluorinated cationic membrane Nafion 117 of Dupont and the reference electrode was a saturated calomel electrode model TR-100 from Tacussel.

The products employed for obtaining the different solutions were HBF_4 (from FLUKA, 50% purity), PbO (from Panreac PRS, 98%), H_3BO_3 (from Panreac PRS), NaOH (from Panreac PRS), H_2SO_4 (from Panreac PRS) and hydrogen N-50 from L'Air Liquide. Analyses of Pb^{2+} solutions were analysed with an ICP Perkin-Elmer Optima 3000.

The HDE anode was fabricated in the following manner: A fixed amount of 10% in weight platinum catalysed Vulcan XC-72 carbon (supplied by ETEK) is dispersed with a PTFE emulsion 50% w/w and applied onto a thin sheet of Toray Paper TGPH-090 (supplied by ETEK). Next, the composite structure was dried at 110°C under pressure (10 kgf cm^{-2}) and sintered at a maximum temperature of 350°C.

4. Results and discussion

4.1. Voltammetric study

Fig. 3A shows a voltammogram obtained in the potential range from −0.1 to −1.2 V. The voltammetric profile shows a cathodic peak at −0.53 V and its anodic counterpart at −0.15 V approximately. These peaks are related to lead electrodeposition and electrodissolution, respectively. The voltammogram clearly shows that a copper electrode can be used as cathode for lead electrodeposition in this electrolyte. Hydrogen evolution does not appear until potentials more negative than −1.2 V showing that even at the initial stage of the electrodeposition, the CE will be very high. Once the lead deposit is formed, the hydrogen evolution is strongly hindered. Thus, the scrapping of the

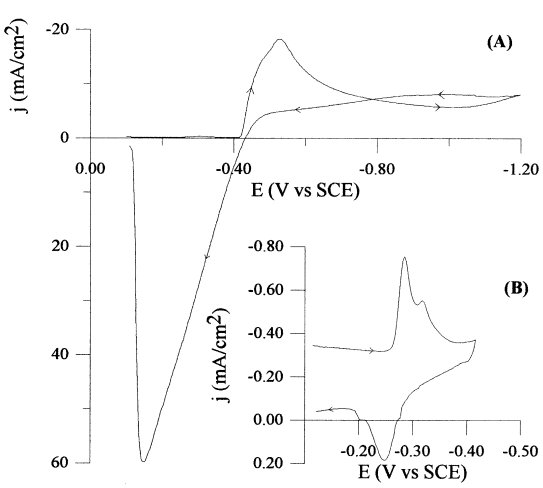

Fig. 3. (A) Voltammetric curve of lead deposit on copper in acid fluoborate medium. (B) Voltammetric curve registered in the UPD region. Electrolyte composition and scan rate were in both curves 0.48 M HBF_4 + 0.16 M H_3BO_3 + 0.048 M Pb^{2+} and 0.05 V/s, respectively.

Table 1
Different stages in electrodeposition of lead

Potential region	Deposition process stage
−0.10/−0.35 V vs. SCE	UPD
−0.35/−0.475 V vs. SCE	Nucleation-controlled region
−0.475/−1.00 V vs. SCE	Diffusion-controlled region
−1.00/−1.20 V vs. SCE	Dendritic growth region

cathode for obtaining metallic lead does not cause a decrease in the CE. The voltammogram can be divided into four different regions that correspond to different stages of the reaction. These are shown in Table 1 and they are attributed to the underpotential deposition zone, the nucleation zone, the diffusion-controlled zone and the dendritic growth zone. Transition among these phases is obviously gradual. Thus, potential values given in Table 1 are only approximate.

The morphology of electrodeposited lead in the different zones was examined by the use of SEM. The deposits were obtained during a negative cycle with an initial potential of −0.1 V. The final potential E_f was chosen depending on each deposition stage required.

4.1.1. UPD process

The existence of a UPD process of lead on copper is a known phenomenon. This has been studied previously in different electrolytes [18,19]. The voltammogram of the UPD process of our experimental conditions is shown as an inset in Fig. 3B. The curve shows two cathodic peaks at −0.28 and −0.31 V, and an anodic peak at −0.24 V with a shoulder at −0.20 V.

4.1.2. Deposition process controlled by nucleation

The voltammogram of this stage that shows the characteristic profile of an electrodeposition process can be seen in Fig. 4. Such processes cause very peculiar voltammograms, which were studied intensely in the 1980s [20–22]. For example, on the positive going scan, there is a potential range where the cathodic current density is higher than on the negative going scan. This unusual feature arises because of the need to form nuclei of the electrodeposited metal phase on the electrode surface. On the other hand, the positive going scan shows a sharp anodic peak due to the oxidation of the electrodeposited metal layer.

Bulk lead deposition starts approximately at −0.43 V. The negative going scan is reversed at −0.45 V. A typical nucleation loop appears caused by the existence of a nucleation overvoltage due to the sluggishness of nuclei formation. After this, the current turns anodic, and the dissolution of deposited lead starts. Current density grows until the potential reaches −0.38 V and then, suddenly, diminishes due to the removal of the deposit. Fig. 5 shows a microphotograph of a deposit obtained with $E_f = -0.44$ V. Small lead crystallites can be seen whose composition was confirmed by means of EDX analysis.

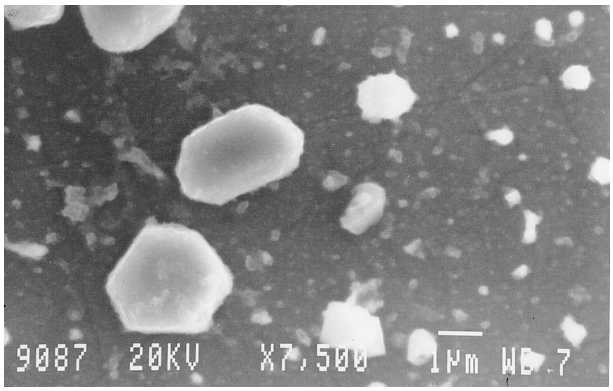

Fig. 5. Microphotography of a Pb deposit formed after the potential scan to −0.44 V at 0.05 V/s. Electrolyte composition: 0.48 M HBF_4 + 0.16 M H_3BO_3 + 0.048 M Pb^{2+}.

4.1.3. Deposition process controlled by diffusion

After the cathodic peak at −0.53 V, the process is controlled by diffusion of Pb^{2+} from the bulk solution.

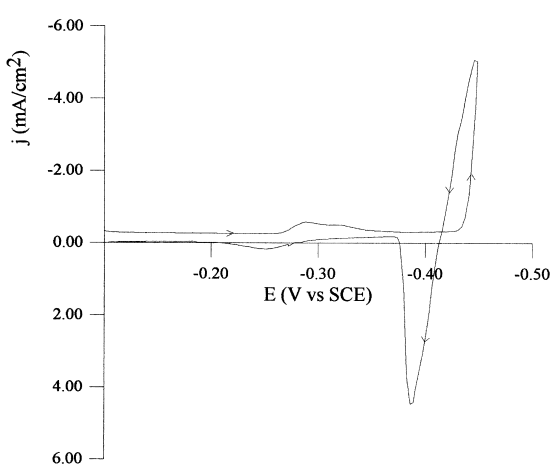

Fig. 4. Voltammetric curve registered in the nucleation-controlled region. Electrolyte composition: 0.48 M HBF_4 + 0.16 M H_3BO_3 + 0.048 M Pb^{2+}. Scan rate: 0.05 V/s.

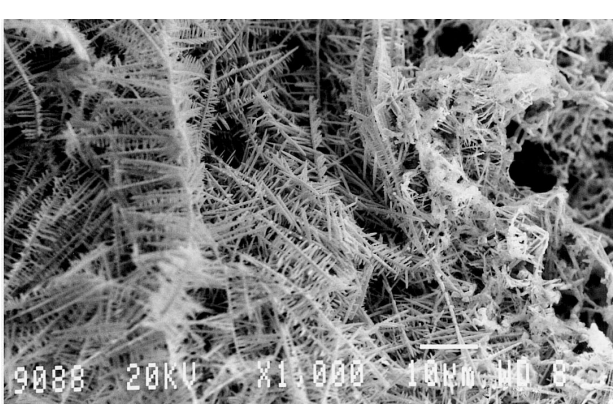

Fig. 6. Microphotography of a Pb deposit formed after the potential scan to −1.2 V at 0.05 V/s. Electrolyte composition: 0.48 M HBF_4 + 0.16 M H_3BO_3 + 0.048 M Pb^{2+}.

Table 2
Influence of current density in CE% of lead deposit. Catholyte composition: 0.16 M H_3BO_3 + 0.048 M PbO + 0.48 M HBF_4, temperature 60°C and catholyte flow: 100 l/h

% Theoretical charge passed	Current density (mA/cm^2)		
	10	100	150
	CE% Pb	CE% Pb	CE% Pb
25	97.8	86.0	81.0
50	98.2	93.2	89.2
75	98.2	94.7	83.7
100	93.0	83.9	73.1

Table 4
Influence of catholyte flow in CE% of lead deposit. Catholyte composition: 0.16 M H_3BO_3 + 0.048 M PbO + 0.48 M HBF_4, temperature 60°C and current density: 100 mA/cm^2

% Theoretical charge passed	Catholyte flow (l/h)	
	10	100
	CE%Pb	CE%Pb
25	61.2	86.0
50	78.4	93.2
75	83.6	94.7
100	71.3	83.9

The diffusion control of the deposition reaction was checked by registering the voltammogram of lead deposition at different scan rates, following the peak current density. Registered microphotographs at $E_f = -0.65$ V showed that lead deposit was very uniform and covered the entire electrode surface.

4.1.4. Deposition process controlled by dendritic growth

The potential interval from −0.8 to −1.2 V corresponds to the dendritic growing zone and the current loop that appears (Fig. 3A) in this interval is due to the increase of the surface area caused by the dendritic zone. Fig. 6 shows a microphotograph with $E_f = -1.2$ V in which well developed dendritic growth can be seen.

4.2. Electrochemical reactor experiments

4.2.1. Optimisation of the reaction of lead deposition

In order to obtain lead deposits with good physical characteristics and high CEs, the deposition process was optimised. The initial experimental variables selected were: catholyte composition 0.16 M H_3BO_3 + 0.048 M PbO + 0.48 M HBF_4, *j*: 100 mA/cm^2, temperature 60°C and catholyte flow: 100 1/h (3.9 cm/s). The anode was a DSA-O_2 and the anolyte was a 1 M NaOH solution. In order to examine the influence of each variable on the deposit reaction, only one of them is changed and the influence of this change is studied. In order to calculate the partial CEs and EC, during the experiments, Pb^{2+} concentration in catholyte and the volume of H_2 evolved at the cathode were measured.

4.2.1.1. Influence of current density. Table 2 shows CE% values at three different current densities. It can be seen that, as expected, an increase in current density causes a decrease in CE% of the deposition reaction.

The obtained lead deposits had good adherence, although their physical properties were very different. A higher working current density gave rise to spongier deposits. Owing to the ''edge effect'', the deposits grow preferentially at the edges. This effect was more important at high current densities.

4.2.1.2. Influence of temperature. Table 3 shows CE% values for four different temperatures. The results obtained show that an increase in the temperature causes an improvement in the CE%. However, the morphology of the deposited lead does not change in a noticeable way.

4.2.1.3. Influence of catholyte flow. Data of CE% at different catholyte flows are shown in Table 4. An increase in catholyte flow gives rise to an improvement in the CE% of the lead deposition reaction caused by an increase of the mass transport of Pb^{2+} to the electrode. The morphology of the deposit does not change.

4.2.1.4. Influence of H^+ concentration. Table 5 shows CE% values at three different fluoboric acid concentrations. As expected, the increase in fluoboric acid concen-

Table 3
Influence of temperature in CE% of lead deposit. Catholyte composition: 0.16 M H_3BO_3 + 0.048 M PbO + 0.48 M HBF_4, current density 100 mA/cm^2 and catholyte flow: 100 l/h

% Theoretical charge passed	Temperature (°C)			
	30	40	50	60
	CE% Pb	CE% Pb	CE% Pb	CE% Pb
25	67.3	75.9	81.1	86.0
50	83.1	87.2	90.0	93.2
75	83.8	88.3	93.4	94.7
100	73.0	75.1	80.2	83.9

Table 5
Influence of HBF_4 concentration in CE% of lead deposit. Catholyte composition: 0.16 M H_3BO_3 + 0.048 M PbO + variable HBF_4, temperature 60°C, current density 100 mA/cm^2 and catholyte flow: 100 l/h

% Theoretical charge passed	HBF_4 concentration (M)		
	0.18	0.48	0.68
	CE% Pb	CE% Pb	CE% Pb
25	98.2	86.0	77.9
50	97.6	93.2	78.6
75	98.1	94.7	90.1
100	90.3	83.9	78.9

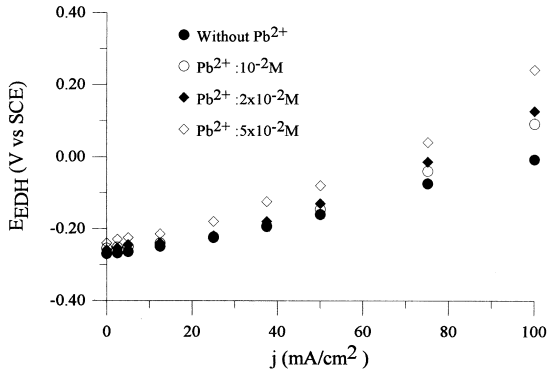

Fig. 7. Voltage–current density curves for a platinum-catalysed hydrogen diffusion electrode in different electrolytes. Electrolyte composition: 0.48 M HBF_4 + 0.16 M H_3BO_3 + 0.048 M Pb^{2+}.

tration causes an increase in the H_2 generation. This produces a spongier deposit with tendency to buoyancy.

4.2.2. Utilisation of an HDE anode

As we stated previously, to save energy, the O_2 evolution reaction can be replaced by the H_2 oxidation reaction that takes place at much more negative potentials, decreasing the cell potential and, therefore, the EC of our process. To do this, the DSA-O_2 anode was replaced by an HDE anode. The first step was to check the influence of Pb^{2+} ions on the HDE behaviour. Fig. 7 shows the curves j–E_{HDE}. The experiments were carried out in a filter press electrochemical reactor with 20 cm^2 geometric area, with no divided compartments. The experimental variables selected were: catholyte composition 0.16 M H_3BO_3 + 0.48 M HBF_4, temperature 60°C and catholyte flow: 100 l/h (3.9 cm/s).

In each experiment, Pb^{2+} concentration in catholyte was changed. Different current densities were used, and the corresponding E_{HDE} values were registered. Fig. 7 shows that an increase in Pb^{2+} concentration causes an increase in the potential of the HDE electrode. This behaviour can be explained as being due to the poisoning of Pt by lead UPD decreasing the rate of the hydrogen oxidation reaction. Thus, the rate of this reaction is decreased and higher potentials are needed to keep the current imposed. This poisoning increases with Pb^{2+} concentration. However, after some seconds, the HDE working potential was constant for all current densities and for long periods of time. To check the HDE behaviour in long-term experiments in the presence of Pb^{2+} ions, tests were done lasting 50 h. During these experiments, Pb^{2+} concentration was constant. At the end of these experiments, E_{HDE} increased less than 50 mV.

Table 6
Experimental conditions of the lead deposit experiments using a DSA-O_2 and a HDE anodes

Geometric Area	20 cm^2 (4×5)
Cathode	Cu
Anode	DSA-O_2 y EDH
Reference electrode	SCE
Catholyte	0.16 M H_3BO_3 + 0.048 M PbO + 0.18 M HBF_4
Anolyte	H_2SO_4 1 M
Separator	Nafion 117
Current density	100 mA/cm^2
Catholyte flow	100 l/h
Anolyte flow	100 l/h
Temperature	60°C

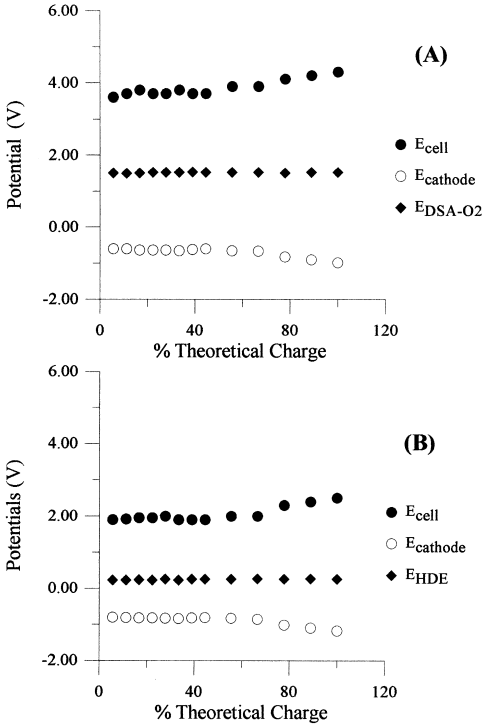

Fig. 8. Representation of $E_{cathode}$, E_{anode} and V_{CELL} vs. % theoretical Charge circulated in the experiments with (A) DSA-O_2 anode (B) HDE anode.

Table 7
E_{anode}, E_{CELL}, CE% and EC values for the experiments shown in Fig. 8

DSA-O_2

% Theoretical charge passed	$E_{DSA\text{-}O_2}$ (V vs. SCE)	E_{CELL} (V)	CE%	EC (kW h/kg_{Pb})
25	1.52	3.7	96.5	0.99
50	1.52	3.9	95.4	1.06
75	1.51	4.1	96.0	1.11
100	1.52	4.3	87.4	1.27

HDE

% Theoretical charge passed	E_{EDH} (V vs. SCE)	E_{CELL} (V)	CE%	EC (kW h/kg_{Pb})	Energy saving using a HDE (%)
25	0.23	1.9	97.4	0.50	49
50	0.25	2.0	95.1	0.54	49
75	0.25	2.3	96.4	0.62	44
100	0.25	2.5	89.9	0.72	43

A comparative study of the use of both anodes, DSA and HDE, during lead electrowinning was carried out for different lead deposition reactions. The experimental conditions are shown in Table 6. Fig. 8A shows the variation of the cathode, anode and cell potentials during the deposition reaction when a DSA-O_2 anode was used. Fig. 8B shows the same parameters when an HDE anode was employed. A substantial decrease in cell potential of approximately 1.8 V is obtained when the latter anode is used. Table 7 shows the values of E_{anode}, V_{CELL}, current efficiency (CE%) and EC for different percentages of the theoretical charge passed together with the energy saving. Table 7 clearly shows that the substitution of the traditionally employed DSA-O_2 anode by an HDE causes an important decrease in the cell voltage and consequently, an important energy saving. This decrease is due to two main reasons. On one hand, the HDE working potential is approximately 1.3 V lower than the DSA-O_2 working potential. On the other hand, the use of an HDE allows the use of a non-divided cell with the consequent decrease in the ohmic drop of the cell.

5. Conclusions

The CE of lead deposition increases when the working current density and H^+ concentration diminish and is higher when catholyte flow and temperature increase.

The use of an HDE anode in place of a DSA-O_2 shows the following advantages. First, it allows to work without separated compartments. In this way, the investment cost is lower. Second, there is a decrease of approximately 45% in the cell voltage at 100% of theoretical charge passed that means that 45% of energy saving is obtained (the CE is not changed). Nevertheless, to calculate the real saving, the value of the H_2 used as feed in the HDE must be taken into account.

As expected, the replacement of the DSA-O_2 anode by an HDE does not affect the efficiency of the deposition reaction, as expected, neither does it influence the physical properties of the deposit.

References

[1] K.D. Libsch, M.E. Erneta, Secondary Lead Processing Current Status, SME-AIME Fall Meeting, St. Louis, MO, 1977, pp. 19–21.
[2] J.H. Trash, Maintenance free batteries effects on the recycling industry, Recycl. Today 16 (1978) 36–40.
[3] R.D. Prengaman, H.B. McDonald, Lead–Zinc 90, in: T.S. Mackey, R.D. Prengaman (Ed.), TMS, Warrendale, PA, 1990.
[4] E.R. Cole, A.Y. Lee, D.L. Paulson, Electrolytic method for recovery of lead from scrap batteries, Bur Mines Report R1 8602, Washington, DC, U.S. Bureau of Mines, 1981.
[5] E.R. Cole, A.Y. Lee, D.L. Paulson, Electrolytic method for recovery of lead from scrap batteries scale up study, Bur Mines Report R1 8857, Washington, DC, U.S. Bureau of Mines, 1984.
[6] E.R. Cole, A.Y. Lee, D.L. Paulson, Recovery of lead from battery sludge by electrowinning, J. Met., August (1983) 42–46.
[7] E.R. Cole, A.Y. Lee, D.L. Paulson, Update on recovering lead from scrap batteries, J. Met., February (1985) 79–83.
[8] G. Diaz, M.L. Abrantes, A. Aldaz, D. Andrews, J. van Erkel, R. Couchinho, Lead recovery from lead oxide secondaries, Brite Euram Programme, Contract no. BRE2-CT9-0119, 1996.
[9] M. Maja, N. Penazzi, M. Baudino, M.V. Ginatta, Recycling of lead/acid batteries: the Ginatta Process, J. Power Sources 31 (1990) 287–294.
[10] T.M. Dobrev, S.R. Rashkov, Investigation of processes occurring during the electrodeposition of lead: Part II. Electrowinning of lead, Bulg. Chem. Commun. 25 (1993) 215–226.
[11] A.J. Appleby, F.R. Foulkes, Fuel Cell Handbook, Van Nostrand Reinhold, 1989.
[12] K. Kordesch, G. Simader, Fuel Cells and Their Applications, VCH, 1996.
[13] V. Plzak, Modern Aspects of Electrochemistry, Vol. 26, Plenum, 1994.
[14] N. Furuya, N. Mineo, High speed zinc electrowinning using a hydrogen gas-diffusion electrode, J. Appl. Electrochem. 20 (1990) 475–478.
[15] R.J. Allen, P.C. Foller, R.J. Vora, R.T. Bombard, M. de Marinis, Full scale hydrogen anodes for immersed tank electrowinning, Journal of Minerals, Metals and Materials, March (1993) 49–53.
[16] V. Nikolova, I. Nikolov, T. Vitanov, Gas-diffusion electrodes catalysed with tungsten carbide as anodes for nickel electrowinning, J. Appl. Electrochem. 17 (1991) 313–316.
[17] E. Expósito, A. Sáez, E. Herrero, A. Aldaz, Use of a hydrogen diffusion electrode in the electrochemical removal of lead from effluents of lead electrowinning processes, Water Environ. Res. 70 (1998) 306–315.
[18] M. Girgis, E. Ghali, A. Wieckowski, Electrochemical studies of lead deposition from acidic ammonium acetate solutions on different substrates, Electrochim. Acta 31 (1986) 681–689.
[19] M. Girgis, E. Ghali, Electrochemical phenomena in aqueous electrowinning of lead, J. Appl. Electrochem. 17 (1987) 1234–1245.
[20] S. Fletcher, Some recent developments in electrochemical nucleation-growth-collision theory, J. Electroanal. Chem. 118 (1981) 419–432.
[21] D.D. McDonald, Transients Techniques in Electrochemistry, cap. 6, Plenum, New York, 1977.
[22] S. Fletcher, C.S. Haliday, D. Gates, M. Westcott, T. Lwin, G. Nelson, The response of some nucleation growth processes to triangular scans of potential, J. Electroanal. Chem. 159 (1983) 267–285.